

Figure S1: Schematic diagram of Coproporphyrin (CP) model in rat and mouse. The model includes three compartments – Plasma, Liver, and Intestine. The numbers represent the processes that are modeled for CP metabolism. 1, Synthesis of CP-I/III from erythrocytes. 2, Hepatic synthesis of CP-I/III 3, Oatp-mediated transport of CP-I/III from plasma to liver. 4, Diffusion-mediated transport of CP-I/III from plasma to liver. 5, Mrp3 mediated transport of CP-I/III from liver to plasma. 6, Mrp2 mediated CP-I/III transport from the liver to the intestine. 7, Non-Mrp2 mediated CP-I/III transport from liver to plasma. 8, Enterohepatic circulation of CP-I/CP-III from intestine to plasma 9, Fecal elimination of CP-I/CP-III. 10, Renal elimination of CP-I/CP-III.

Table S1. Key model parameters used in rat and mouse CP models.

Parameter Name	Description	Value (Rat model)	Value (Mouse model)	Unit	Reference
$k_{m,Oatp,CP-I}$	Affinity constant of CP-I for Oatp	1.66	1.66	μM	[9]
$k_{m,Mrp2,CP-I}$	Affinity constant of CP-I for Mrp2	7.7	7.7	μM	[10]
$k_{m,Mrp3,CP-I}$	Affinity constant of CP-I for Mrp3	3.75	3.75	μM	[11]
$k_{m,Oatp,CP-III}$	Affinity constant of CP-III for Oatp	2.44	2.44	μM	[9]
$k_{m,Mrp2,CP-III}$	Affinity constant of CP-III for Mrp2	7.7	7.7	μM	[10]
$k_{m,Mrp3,CP-III}$	Affinity constant of CP-III for Mrp3	3.75	3.75	μM	[11]
$v_{CP-I,Syn}$	CP-I extrahepaic synthesis rate	0.166	0.0229	nM/min	Computed
$v_{CP-I,hepaticSyn}$	CP-I hepatic synthesis rate	0.032	0.0077	nM/min	Computed
$v_{CP-III,Syn}$	CP-III extra hepatic Synthesis rate	0.896	0.0785	nM/min	Computed
$v_{CP-III,hepaticSyn}$	CP-III hepatic synthesis rate	0.175	0.0263	nM/min	Computed
Liver volume	Volume of liver	0.01	0.0018	Litre	[34]
Plasma volume	Volume of plasma	0.007	0.002	Litre	[34]
Intestinal volume	Volume of intestine	0.011	0.002	Litre	[34]

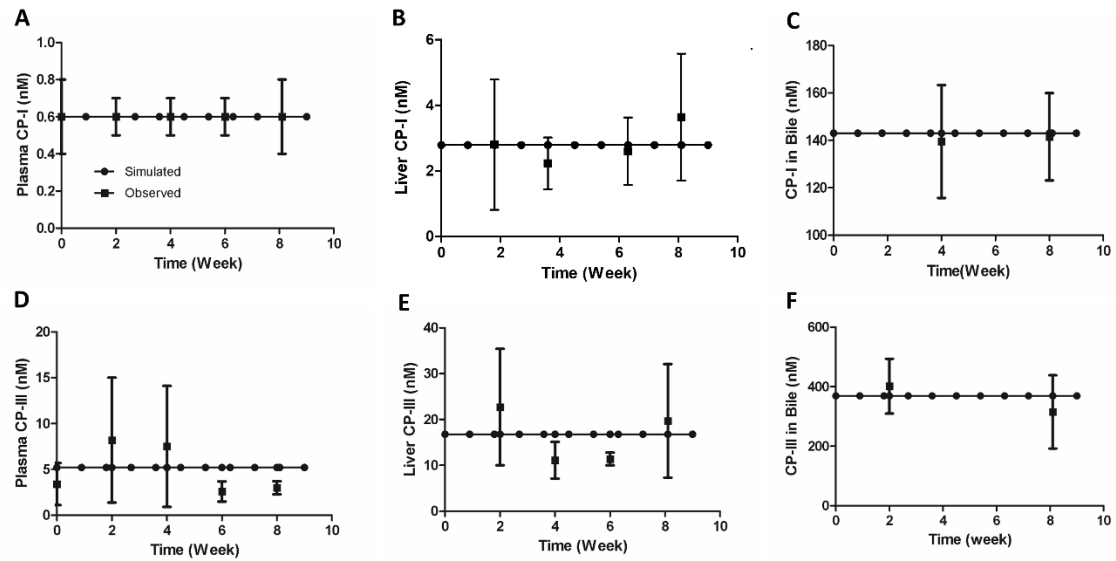


Figure S2: Comparison of model simulated steady states with observed data. (A) Plasma CP-I, (B) Liver CP-I, (C) CP-I in bile, (D) Plasma CP-III, (E) Liver CP-III, (F) CP-III in Bile.

Symbols, the continuous line represents simulated data. Experimental data with error bars (mean \pm SEM) represent observed data. CP-I, Coproporphyrin-I; CP-III, Coproporphyrin-III

Table S2: Model simulated steady states values in mice compared with observed result.

Model Variables	Simulation	Observed [15]
Plasma CP-I (nM)	0.14	0.14±0.02
Plasma CP-III (nM)	0.57	0.57±0.1
Liver CP-I (nM)	0.6	NA
Liver CP-III (nM)	1.57	NA
Bile CP-I (nM)	32	NA
Bile CP-III (nM)	43	NA
CP-I urinary secretion (nmol/h/kg)	0.012	0.0123±0.001
CP-III urinary secretion (nmol/h/kg)	0.034	0.034±0.006

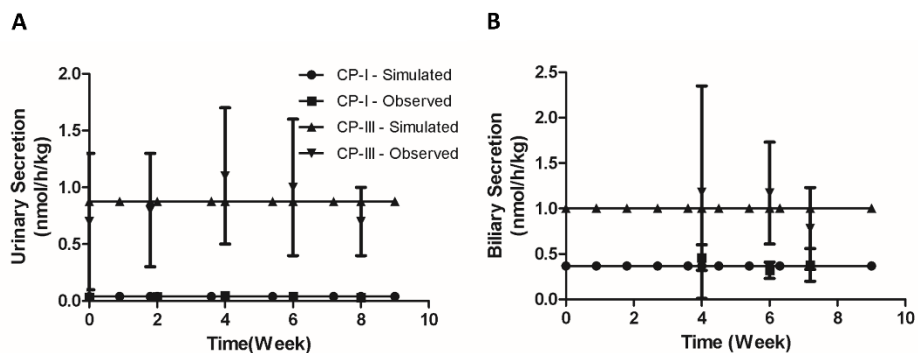


Figure S3: Comparison of model simulated renal and biliary secretion with observed data. (A) CP-I and CP-III urinary secretion (B) CP-I and CP-III biliary secretion.

Symbols, continuous line represents simulated data. Experimental data with error bars (mean \pm SEM) represent observed data. CP-I, Coproporphyrin-I; CP-III, Coproporphyrin-III

Table S3: Model simulated biliary excretion ratio (CP-III/CP-I) with an intravenous infusion with the same and different proportions of CP-I and CP-III.

CP-I infusion rate (µg/h)	CP-III infusion rate (µg/h)	Simulation	Observed [31]
60	60	2.5	2
30	60	1.5	1
60	30	4.6	4.2

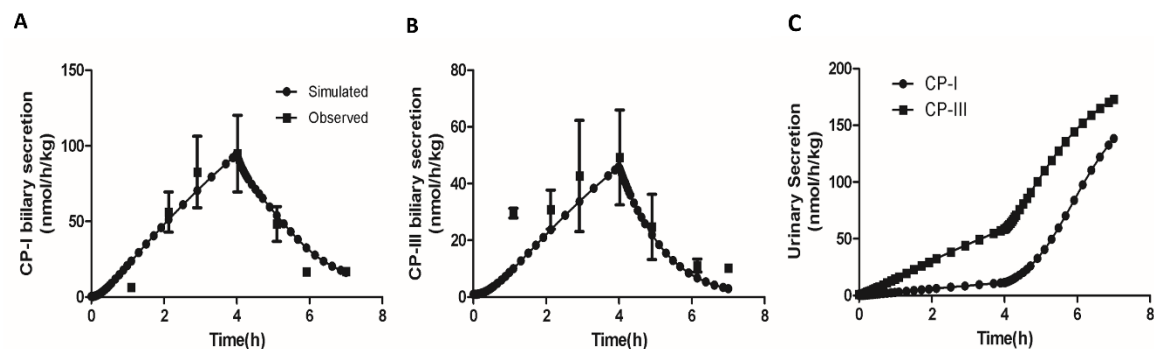


Figure S4 : Model simulation showing the effect of concomitant infusion of bromosulphophthalein (BSP) with equal amounts of CP-I and CP-III. (A) CP-I biliary secretion (B) CP-III biliary secretion, (C) CP-I, and CP-III biliary secretion. Data was extracted using the WebPlotDigitizer tool (URL: <https://apps.automeris.io/wpd/>). Experimental data [30] with error bars (mean \pm SD) represent observed data. CP-I, Coproporphyrin-I ; CP-III, Coproporphyrin-III

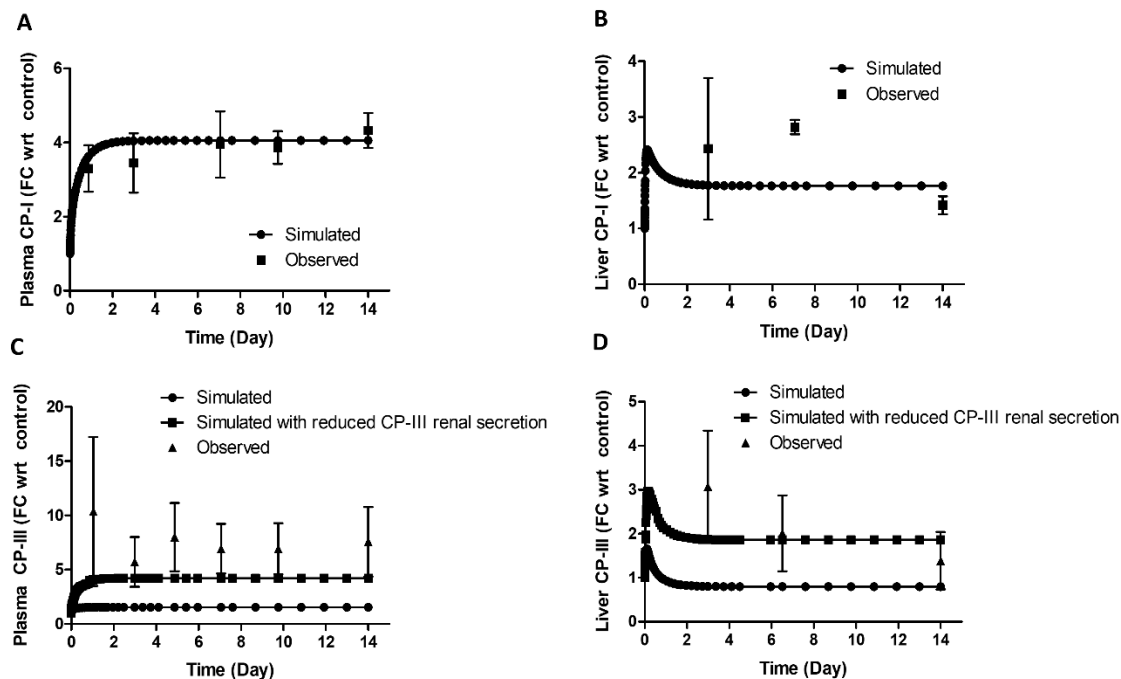


Figure S5: Comparison of model simulated plasma and liver CP-I and CP-III and with observed data in BDL rat. (A) Plasma CP-I, (B) Liver CP-I, (C) Plasma CP-III, (D) Liver CP-III. Symbols, continuous line represents simulated data. Data was extracted using the WebPlotDigitizer tool (URL: <https://apps.automeris.io/wpd/>) Experimental data [11] with error bars (mean \pm SEM) represent observed data. CP-I, Coproporphyrin-I; CP-III, Coproporphyrin-III, FC wrt control, Fold change with respect to control

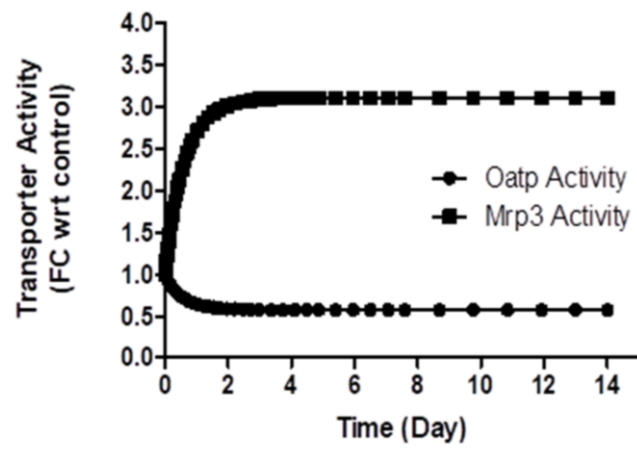


Figure S6: Model simulated change in transporter activity during bile-duct ligation (BDL) in rat.
Symbol, FC wrt control, Fold change with respect to control.

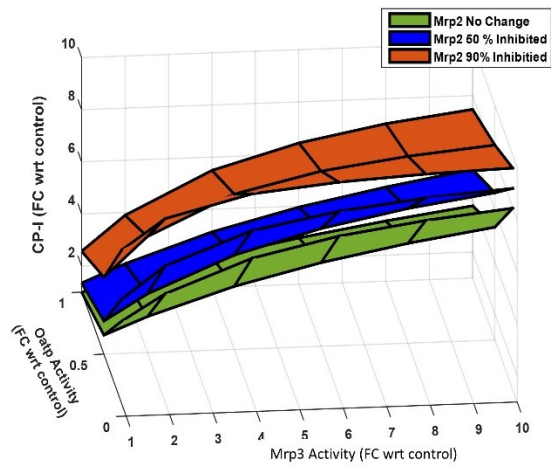


Figure S7: Steady-state continuation analysis showing the impact of different transporters (Oatp, Mrp3, and Mrp2) on plasma CP-I level. Symbol, FC wrt control, Fold change with respect to control.

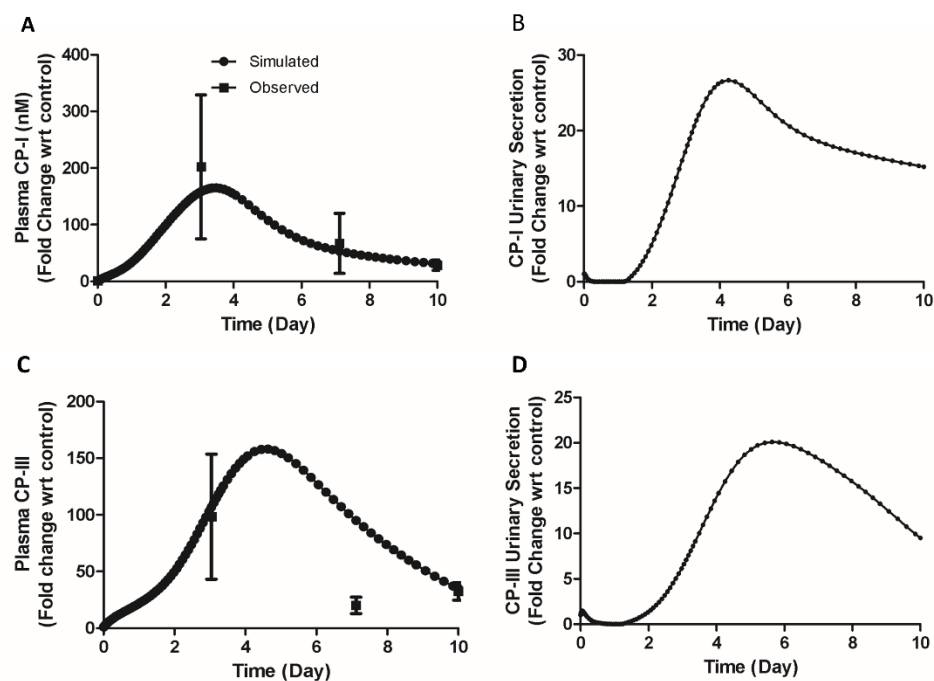


Figure S8: Comparison of model simulated plasma CP-I and CP-III with observed data and simulated biliary secretion CP-I and CP-III. (A) Plasma CP-I, (B) CP-I urinary secretion, (C) Plasma CP-III, (D) CP-III urinary secretion. Symbols, continuous line represents simulated data. Experimental data [11] with error bars (mean \pm SEM) represent observed data. CP-I, Coproporphyrin-I; CP-III, Coproporphyrin-III

Table S4: Model simulation results of CP-I and CP-III disposition in Oatp KO mice; * Simulations done with increased hepatic CP-III synthesis

Model Variables	Simulation A	Simulation B*	Observed [15]
Plasma CP-I (nM)	1.01	1.01	0.98±0.03
Plasma CP-III (nM)	5.30	8.84	8.76±0.92
CP-I urinary secretion (nmol/h/kg)	0.08	0.08	0.15±0.05
CP-III urinary secretion (nmol/h/kg)	0.25	0.43	0.61±0.17

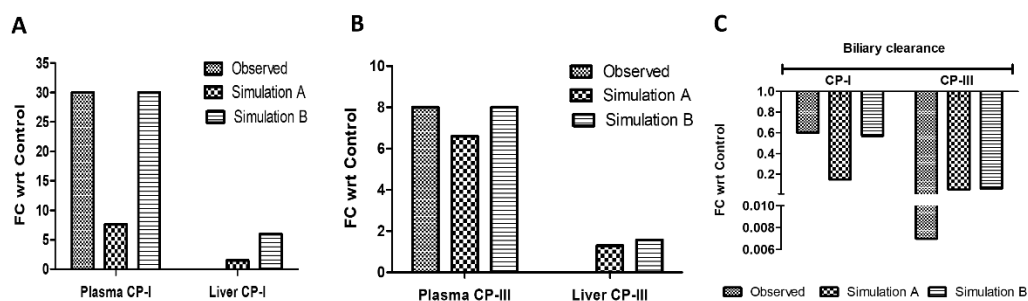


Figure S9: Comparison of model-simulated and observed data in TR- rats. [33]. Simulation details are given in the manuscript. (A) Plasma CP-I and Liver CP-I, (B) Plasma CP-III, (C) CP-I and CP-III biliary secretion. FC, fold change; CP-I, Coproporphyrin-I ; CP-III, Coproporphyrin-III